Last time | Considered scattering in impact parameter space, obtaining

$$\sigma_{tot} = 2\int d^2b\,[1 - \mathrm{Re}\,\$(s,\underline{b})]$$

$$\sigma_{el} = \int d^2b\,|1 - \$(s,\underline{b})|^2$$

$$\sigma_{inel} = \int d^2b\,[1 - |\$(s,\underline{b})|^2]$$

at high energies $\mathrm{Re}\,\$ \geq 0 \Rightarrow \sigma_{tot} \leq 2\underbrace{\int d^2b}_{\pi R^2}$

$\Rightarrow$ $\sigma_{tot} \leq 2\pi R^2$ ~ black disk limit.

as $R \sim \ln s \Rightarrow$ $\sigma_{tot} \leq \frac{\#}{m_\pi^2}\ln^2 s$ ~ Froissart bound

Dipole Picture of DIS (cont'd)

rest frame of proton

$q^\mu = (q^+, -\frac{Q^2}{q^+}, \underline{0})$

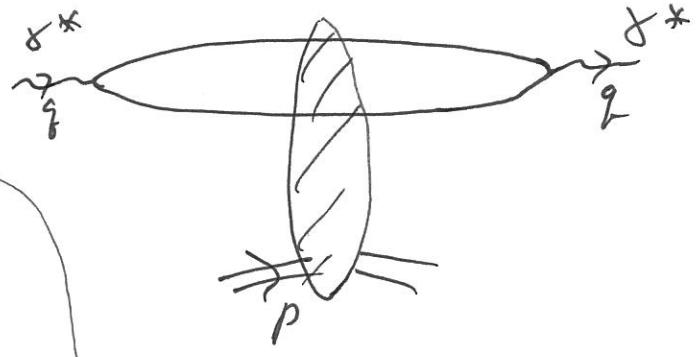

$$\sigma_{tot}^{\gamma^* A}(x,Q^2) = \int \frac{d^2x_\perp}{4\pi}\int_0^1 \frac{dz}{z(1-z)} \cdot |\Psi^{\gamma^* \to q\bar{q}}(\underline{x},z)|^2\, \sigma_{tot}^{q\bar{q}A}(\underline{x},Y)$$

, $Y = \ln\frac{1}{x}$

$\sim \ln(s x^2)$

coherence length of the quark loop:

$$l_{coh} = x^+ \simeq \frac{2}{|q^-|} = \frac{2q^+}{Q^2} = \left| \text{as } x = \frac{Q^2}{2p\cdot q} \right| = \frac{2q^+}{\underbrace{2x\, p\cdot q}_{\simeq \frac{1}{2} q^+ \cdot m}} \simeq \frac{2}{mx}$$

$$\Rightarrow \boxed{l_{coh} \simeq \frac{2}{mx}} \quad \Rightarrow \text{small } x \text{ loop lives longer!}$$

4

Dipole approach to high parton density QCD

We are now ready to present more recent developments in high energy QCD. We will consider DIS in the rest frame of a proton or a nucleus. In this frame a virtual photon fluctuates into a quark–antiquark pair, which, in turn, hits the proton or nuclear target. We argue that quark–antiquark dipoles are convenient degrees of freedom for high energy scattering in QCD. We will present a simple model of DIS on a nucleus, due to Glauber, Gribov, and Mueller, in which the $q\bar{q}$ dipole rescatters multiple times on a nuclear target consisting of independent nucleons. We then include quantum corrections to this multiple-rescattering picture: we argue that the initial $q\bar{q}$ dipole may develop a cascade of gluons before hitting the target nucleus. In the large-N_c limit the cascade is described by Mueller's dipole model. When applied to DIS the dipole cascade resummation leads to the Balitsky–Kovchegov (BK) nonlinear evolution equation. We describe approximate analytical and exact numerical solutions of the BK equation and show that it resolves both problems of BFKL evolution: BK evolution is unitary and has no diffusion into the IR. It generates a saturation scale Q_s that grows with energy, justifying the use of perturbative QCD. We conclude the chapter by presenting the Bartels–Kwiecinski–Praszalowicz (BKP) evolution equation for multiple reggeon exchanges, along with the evolution equation for (C-odd) odderon exchange.

4.1 Dipole picture of DIS

Let us begin by considering DIS in the rest frame of the proton or nucleus. While many conclusions in this chapter may also apply to proton DIS, in the strict sense our results would be justified only for DIS on a large nucleus since such a nucleus has a large atomic number parameter A allowing us to make the approximations we will need below. We will therefore only talk about DIS on a nuclear target.

Without any loss of generality we can choose a coordinate axis such that the momentum of the virtual photon is given by

$$q_\mu = \left(q_+, -\frac{Q^2}{q_+}, 0_\perp\right) \tag{4.1}$$

in the $(+, -, \perp)$ light cone notation. The light cone momentum of the virtual photon q_+ is very large (since the (high) photon–nucleus center-of-mass energy is $\hat{s} = mq^+$), so that its

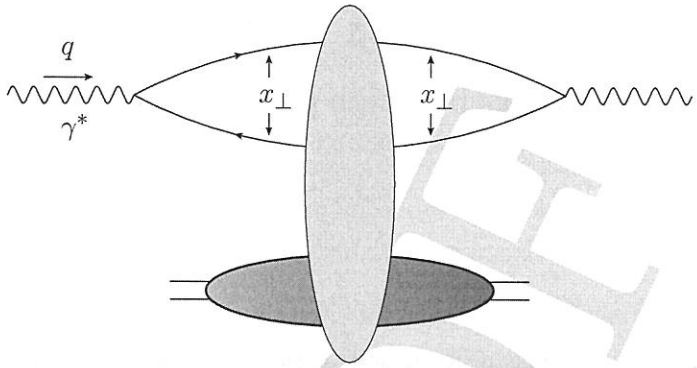

Fig. 4.1. Forward scattering amplitude for DIS on a proton or nuclear target in the rest frame of the target: the virtual photon splits into a $q\bar{q}$ pair which then interacts with the target. The interaction is depicted by the vertical oval. For simplicity the electron that emits the virtual photon is not shown.

coherence length in the longitudinal plus direction (see Sec. 2.3 above),

$$x^+ \approx \frac{2}{|q^-|} = \frac{2q^+}{Q^2}, \tag{4.2}$$

is much larger than the size of the nucleus. If the virtual photon fluctuates into a quark–antiquark pair, the typical lifetime of such a $q\bar{q}$ fluctuation would also be much longer than the nuclear diameter. Therefore, a DIS process in the nuclear rest frame occurs when a virtual photon fluctuates into a $q\bar{q}$ pair (which we will also refer to as a color dipole or simply a dipole); the $q\bar{q}$ pair proceeds to interact with the target (Gribov 1970, Bjorken and Kogut 1973, Frankfurt and Strikman 1988). The forward scattering amplitude for the process is pictured in Fig. 4.1, with the $q\bar{q}$ dipole–nucleus interaction represented by the vertical oval. This is the dipole picture of DIS (Kopeliovich, Lapidus, and Zamolodchikov 1981, Bertsch *et al.* 1981, Mueller 1990, Nikolaev and Zakharov 1991). Note that while the topology of the DIS diagram in Fig. 4.1 is the same as for DIS in the IMF, shown in Fig. 2.2, the time-ordering of the interactions is different in the two figures.

The interaction of a virtual photon with a nucleus can be viewed as a two-stage process: the virtual photon decays into a colorless dipole consisting of a quark and an antiquark and the colorless dipole travels through the nucleus. However, this separation between the time scale for the photon to decay into the $q\bar{q}$ pair and the interaction time is not the only advantage of the dipole picture. Another important simplification comes from the fact that in high energy scattering a colorless dipole, with transverse size $x_\perp$, does not change its size during the interaction and therefore the S-matrix of the interaction is diagonal with respect to the transverse dipole size (Zamolodchikov, Kopeliovich, and Lapidus 1981, Levin and Ryskin 1987, Mueller 1990, Brodsky *et al.* 1994). Indeed, while the colorless dipole is traversing the target, the distance $x_\perp$ between the quark and antiquark can only

vary by an amount

$$\Delta x_\perp \approx R\frac{k_\perp}{E} \tag{4.3}$$

where $E \sim q^0$ denotes the energy of the dipole in the laboratory frame (the target rest frame), R is the longitudinal size of the target, and $k_\perp$ is the relative transverse momentum of the $q\bar{q}$ pair acquired through interaction with the target. In Eq. (4.3) $k_\perp/E$ is the relative transverse velocity of the quark with respect to the antiquark. From Eq. (4.3) we can see already that the change in the dipole size is suppressed by a power of the energy E and is therefore small. To quantify this better let us first remember the definition of Bjorken x, given in (2.2):

$$x = \frac{Q^2}{2P\cdot q} = \frac{Q^2}{mq^+} \approx \frac{Q^2}{2mE}. \tag{4.4}$$

Using Eq. (4.4) in Eq. (4.3) along with the uncertainty principle $Q \approx k_\perp \approx 1/x_\perp$ yields

$$\frac{\Delta x_\perp}{x_\perp} \approx 2mxR = \frac{4R}{l_{coh}} \ll 1, \tag{4.5}$$

where $l_{coh} = 2/(mx)$ is the coherence length of the dipole fluctuation (see Eq. (2.56)). We thus see that at small $x \ll 1/(mR)$, when the dipole interacts with the whole nucleus coherently in the longitudinal direction, the transverse recoil of the quark and the antiquark are negligible compared with the size of the dipole. Therefore the transverse size of the dipole is invariant in high energy interactions, as indicated in Fig. 4.1.

We conclude that in calculating the total DIS cross section, along with other high energy QCD observables, it is convenient to work in transverse coordinate space. We will therefore adopt a mixed representation: we will use longitudinal momentum space along with transverse coordinate space. Light cone perturbation theory (LCPT) is a very useful tool here again. Using LCPT to calculate the total DIS $\gamma^* A$ cross section we can factorize the diagram in Fig. 4.1 into the square of the light cone wave function $\Psi^{\gamma^*\to q\bar{q}}(\vec{x}_\perp, z)$ for the splitting of a virtual photon into a $q\bar{q}$ dipole and the total cross section for the scattering of a dipole on a target nucleus $\sigma_{tot}^{q\bar{q}A}(\vec{x}_\perp, Y)$, so that

$$\sigma_{tot}^{\gamma^* A}(x, Q^2) = \int \frac{d^2x_\perp}{4\pi}\int_0^1 \frac{dz}{z(1-z)}|\Psi^{\gamma^*\to q\bar{q}}(\vec{x}_\perp, z)|^2 \sigma_{tot}^{q\bar{q}A}(\vec{x}_\perp, Y). \tag{4.6}$$

Here $z = k^+/q^+$, with k^+ the light cone momentum of the quark in the $q\bar{q}$ pair. In general the dipole–nucleus cross section will depend on z too; however, in the eikonal and LLA approximations that we mainly consider below, $\sigma_{tot}^{q\bar{q}A}$ is independent of z. The net rapidity interval for the dipole–nucleus scattering is given by $Y = \ln(\hat{s}x_\perp^2) \approx \ln 1/x$ for $x_\perp \sim 1/Q$.

The reader may have other doubts about the factorization (4.6): after all, the LCPT rules presented in Sec. 1.3 require us to subtract the light cone energy of the incoming state in the energy denominator from each intermediate state's energy. Since the light cone energy of the incoming virtual photon is $q^- = -Q^2/q^+$, it seems that each intermediate state that

we have absorbed into $\sigma_{tot}^{q\bar{q}A}(\vec{x}_\perp, Y)$ should "know" about the photon's energy. However, in the rest frame of the nucleus, q^- is equal to $-Q^2/q^+ \sim 1/\hat{s}$ and is therefore negligibly small compared with the typical minus components of momenta involved in dipole–nucleus interactions. The same would be true for dipole–nucleus scattering: the incoming dipole state would have a negligibly small light cone energy compared with the energies involved in the interaction. Therefore, in our eikonal approximation (up to corrections of order $1/\hat{s}$), we can interchange the negligible light cone energy q^- for the light cone energy of the dipole without changing the answer, thus justifying the factorization of Eq. (4.6). (Note that in calculating the light cone wave function $\Psi^{\gamma^* \to q\bar{q}}(\vec{x}_\perp, z)$ we cannot neglect the light cone energies of the virtual photon and the $q\bar{q}$ dipole, since they are the only terms entering the energy denominator.) Another important assumption is that the light cone energy of the target is not modified until the interaction with the dipole: one can show that the time scale of target fluctuations is much shorter than the lifetime of the dipole. Hence the target does not affect the virtual photon's wave function, since in constructing the latter the same light cone energy of the target enters into both the energies of the intermediate states and the initial-state energy, thus canceling in the energy denominators.

The factorization of Eq. (4.6) is very convenient: it allows us to separate the simple $\gamma^* \to q\bar{q}$ QED process from the strong interaction dynamics contained in $\sigma_{tot}^{q\bar{q}A}(\vec{x}_\perp, Y)$.

Note that the virtual photon may have either transverse or longitudinal polarization. Requiring that the photon polarization satisfies $\epsilon \cdot q = 0$ and imposing $\epsilon_T^2 = -1$ for transverse polarization and $\epsilon_L^2 = 1$ for the longitudinal polarization, we obtain for q^μ, Eq. (4.1), the following polarizations:

$$\epsilon_T^\lambda = (0, 0, \vec{\epsilon}_\perp^\lambda), \tag{4.7a}$$

$$\epsilon_L = \left(\frac{q^+}{Q}, \frac{Q}{q^+}, \vec{0}_\perp\right), \tag{4.7b}$$

with $\vec{\epsilon}_\perp^\lambda$ as given in Eq. (1.54). The polarization vectors (4.7) form a complete basis in the space of possible polarizations, so that the numerator of the photon propagator in the Landau gauge can be decomposed in terms of them as

$$g_{\mu\nu} - \frac{q_\mu q_\nu}{q^2} = -\sum_{\lambda=\pm} \epsilon_{T\mu}^\lambda \epsilon_{T\nu}^{\lambda *} + \epsilon_{L\mu} \epsilon_{L\nu}^*. \tag{4.8}$$

Using the polarizations (4.7) along with Eqs. (2.13) and (2.16) one can separate the total DIS cross section into transverse (T) and longitudinal (L) components (see Halzen and Martin 1984):

$$\sigma_T^{\gamma^* A} = \frac{4\pi^2 \alpha_{EM}}{q^0} W^{\mu\nu} \frac{1}{2} \sum_{\lambda=\pm} \epsilon_{T\mu}^\lambda \epsilon_{T\nu}^{\lambda *} = \frac{4\pi^2 \alpha_{EM}}{q^0} W_1 \tag{4.9a}$$

$$\sigma_L^{\gamma^* A} = \frac{4\pi^2 \alpha_{EM}}{q^0} W^{\mu\nu} \epsilon_{L\mu} \epsilon_{L\nu}^* = \frac{4\pi^2 \alpha_{EM}}{q^0} \left[-W_1 + \left(1 + \frac{\nu^2}{Q^2}\right) W_2\right], \tag{4.9b}$$

with ν as defined in Eq. (2.5) and α_{EM} the fine structure constant. Employing Eqs. (2.18a) and (2.18b), we can rewrite Eqs. (4.9) in the high energy $\nu \gg Q$ limit as expressions for

$4\pi\alpha_{EM} = e^2$

$\pi \sim$ removes $\frac{1}{\pi}$

$\frac{\pi e^2}{q^0} \frac{1}{4\pi m} = \frac{1}{2q^0 2m}$ ~ flux factor

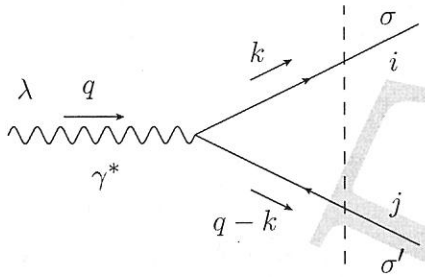

Fig. 4.2. Light cone wave function for a virtual photon fluctuating into a quark–antiquark pair (a dipole). The broken line denotes the intermediate state.

the dimensionless structure functions:

$$F_2(x, Q^2) = \frac{Q^2}{4\pi^2 \alpha_{EM}} \sigma_{tot}^{\gamma^* A} = \frac{Q^2}{4\pi^2 \alpha_{EM}} \left(\sigma_T^{\gamma^* A} + \sigma_L^{\gamma^* A} \right), \tag{4.10a}$$

$$2x F_1(x, Q^2) = \frac{Q^2}{4\pi^2 \alpha_{EM}} \sigma_T^{\gamma^* A}. \tag{4.10b}$$

It is useful to also define the longitudinal structure function F_L, which measures the violation of the Callan–Gross relation (2.44):

$$F_L(x, Q^2) \equiv F_2(x, Q^2) - 2x F_1(x, Q^2) = \frac{Q^2}{4\pi^2 \alpha_{EM}} \sigma_L^{\gamma^* A}. \tag{4.11}$$

Equations (4.10) and (4.11) allow us to find the DIS structure functions using the transverse and longitudinal cross sections, which, with the help of Eq. (4.6), can be found from the dipole–nucleus scattering via

$$\sigma_{T,L}^{\gamma^* A}(x, Q^2) = \int \frac{d^2 x_\perp}{4\pi} \int_0^1 \frac{dz}{z(1-z)} \left| \Psi_{T,L}^{\gamma^* \to q\bar{q}}(\vec{x}_\perp, z) \right|^2 \sigma_{tot}^{q\bar{q}A}(\vec{x}_\perp, Y). \tag{4.12}$$

We have defined the transverse, $\Psi_T^{\gamma^* \to q\bar{q}}(\vec{x}_\perp, z)$, and longitudinal, $\Psi_L^{\gamma^* \to q\bar{q}}(\vec{x}_\perp, z)$, light cone wave functions, which differ by the polarization vector of the incoming virtual photon.

Let us now calculate the light cone wave functions $\Psi_{T,L}^{\gamma^* \to q\bar{q}}(\vec{x}_\perp, z)$ for the quark–antiquark fluctuations of a virtual photon. The diagram is shown in Fig. 4.2, in which the vertical broken line denotes the intermediate state. Using the LCPT rules from Secs. 1.3 and 1.4, we write for the wave functions in momentum space (cf. the calculation in Sec. 2.4.2)

$$\Psi_{T,L}^{\gamma^* \to q\bar{q}}(\vec{k}_\perp, z) = e Z_f \frac{z(1-z)\delta_{ij}}{\vec{k}_\perp^2 + m_f^2 + Q^2 z(1-z)} \bar{u}_\sigma(k) \gamma \cdot \epsilon_{T,L}^\lambda v_{\sigma'}(q-k), \tag{4.13}$$

where σ and σ' are the quark and antiquark helicities, i, j are their colors, m_f is the mass of a quark with flavor f, and Z_f is the quark's electric charge in units of the electron charge e. (Note that q^μ is given in Eq. (4.1).) As mentioned above, we define $z = k^+/q^+$ as the fraction of the photon's light cone momentum carried by the quark.

Starting with the transverse polarization we substitute the polarization vector from Eq. (4.7a) into Eq. (4.13) and evaluate the Dirac matrix element using Appendix A.1, obtaining

$$\Psi_T^{\gamma^* \to q\bar{q}}(\vec{k}_\perp, z) = eZ_f \sqrt{z(1-z)}\, \delta_{ij} \times \frac{(1-\delta_{\sigma\sigma'})\vec{\epsilon}_\perp^{\,\lambda} \cdot \vec{k}_\perp (1-2z-\sigma\lambda) + \delta_{\sigma\sigma'} m_f (1+\sigma\lambda)/\sqrt{2}}{\vec{k}_\perp^2 + m_f^2 + Q^2 z(1-z)}. \quad (4.14)$$

In arriving at Eq. (4.14) we have also used the fact that in two transverse dimensions $\vec{\epsilon}_\perp^{\,\lambda} \times \vec{k}_\perp = -i\lambda \vec{\epsilon}_\perp^{\,\lambda} \cdot \vec{k}_\perp$ for the $\vec{\epsilon}_\perp^{\,\lambda}$ from Eq. (1.54).

Since we are interested in using the virtual photon's wave function in transverse coordinate space in Eq. (4.12), we perform a Fourier transform of Eq. (4.14):

$$\Psi_{T,L}^{\gamma^* \to q\bar{q}}(\vec{x}_\perp, z) = \int \frac{d^2 k_\perp}{(2\pi)^2} e^{i\vec{k}_\perp \cdot \vec{x}_\perp} \Psi_{T,L}^{\gamma^* \to q\bar{q}}(\vec{k}_\perp, z) \quad (4.15)$$

and employ Eq. (A.11) along with $K_0'(z) = -K_1(z)$ to obtain

$$\Psi_T^{\gamma^* \to q\bar{q}}(\vec{x}_\perp, z) = \frac{eZ_f}{2\pi} \sqrt{z(1-z)} \delta_{ij} \Bigg[(1-\delta_{\sigma\sigma'})(1-2z-\sigma\lambda) i a_f \frac{\vec{\epsilon}_\perp^{\,\lambda} \cdot \vec{x}_\perp}{x_\perp} K_1(x_\perp a_f) + \delta_{\sigma\sigma'} \frac{m_f}{\sqrt{2}} (1+\sigma\lambda) K_0(x_\perp a_f) \Bigg], \quad (4.16)$$

where

$$a_f^2 = Q^2 z(1-z) + m_f^2. \quad (4.17)$$

The square of the absolute value of the transverse wave function (4.16), summed over all the outgoing quantum numbers and averaged over the possible polarizations of the incoming transverse photon is (Bjorken, Kogut, and Soper 1971, Nikolaev and Zakharov 1991) given by

$$|\Psi_T^{\gamma^* \to q\bar{q}}(\vec{x}_\perp, z)|^2 = 2N_c \sum_f \frac{\alpha_{EM} Z_f^2}{\pi} z(1-z) \times \left\{ a_f^2 \left[K_1(x_\perp a_f) \right]^2 \left[z^2 + (1-z)^2 \right] + m_f^2 \left[K_0(x_\perp a_f) \right]^2 \right\}. \quad (4.18)$$

To calculate the longitudinal wave function $\Psi_L^{\gamma^* \to q\bar{q}}(\vec{x}_\perp, z)$ we repeat the above steps, now using the longitudinal polarization vector (4.7b) in Eq. (4.13). The transverse momentum space longitudinal wave function is

$$\Psi_L^{\gamma^* \to q\bar{q}}(\vec{k}_\perp, z) = \frac{eZ_f [z(1-z)]^{3/2}\, \delta_{ij} 2Q (1-\delta_{\sigma\sigma'})}{\vec{k}_\perp^2 + m_f^2 + Q^2 z(1-z)}. \quad (4.19)$$

In arriving at Eq. (4.19) we have neglected a term that would have given us a delta function, $\delta^2(\vec{x}_\perp)$, in the transverse coordinate-space wave function; as we will shortly see,

zero-transverse-size dipoles do not interact with the nucleus (they have zero scattering cross section) and so such configurations do not contribute to the DIS structure functions.

Fourier-transforming Eq. (4.19) into transverse coordinate space yields

$$\Psi_L^{\gamma^* \to q\bar{q}}(\vec{x}_\perp, z) = \frac{eZ_f}{2\pi}[z(1-z)]^{3/2}\,\delta_{ij}\,2Q(1-\delta_{\sigma\sigma'})K_0(x_\perp a_f), \tag{4.20}$$

so that the longitudinal wave function squared, again with all summations performed, is (Bjorken, Kogut, and Soper 1971, Nikolaev and Zakharov 1991)

$$|\Psi_L^{\gamma^* \to q\bar{q}}(\vec{x}_\perp, z)|^2 = 2N_c \sum_f \frac{\alpha_{EM} Z_f^2}{\pi} 4Q^2 z^3 (1-z)^3 \left[K_0(x_\perp a_f)\right]^2. \tag{4.21}$$

To obtain the phase-space integral in Eqs. (4.6) or (4.12) we remember that the two-particle momentum phase space given in Eq. (1.82) is (remembering that in our case the quarks are not identical)

$$\int \frac{dz}{2z(1-z)} \frac{d^2k_\perp}{(2\pi)^3}. \tag{4.22}$$

After Fourier-transforming the wave function into transverse coordinate space the integral becomes

$$\int \frac{dz}{2z(1-z)} \frac{d^2x_\perp}{2\pi}, \tag{4.23}$$

in agreement with Eqs. (4.6) and (4.12).

We have now completed the calculation of the QED part of DIS in the dipole picture. Equations (4.18) and (4.21), when used in Eq. (4.12), give us the transverse and longitudinal DIS cross sections, which, in turn, when used in Eqs. (4.10) and (4.11) give us the structure functions. The interesting physics of strong interactions is contained in the dipole–nucleus scattering cross section $\sigma_{tot}^{q\bar{q}A}(\vec{x}_\perp, Y)$: most of this chapter is dedicated to calculating this quantity.

4.2 Glauber–Gribov–Mueller multiple-rescatterings formula

We begin by employing Eq. (3.119a) to rewrite the total dipole–nucleus scattering cross section as

$$\sigma_{tot}^{q\bar{q}A}(\vec{x}_\perp, Y) = 2\int d^2b\, N(\vec{x}_\perp, \vec{b}_\perp, Y), \tag{4.24}$$

where $N(\vec{x}_\perp, \vec{b}_\perp, Y)$ is the imaginary part of the forward scattering amplitude for a dipole of transverse size $\vec{x}_\perp$ interacting with the nucleus at impact parameter $\vec{b}_\perp$ and with net rapidity interval Y. Hence to find the cross section $\sigma_{tot}^{q\bar{q}A}$ we need to calculate $N(\vec{x}_\perp, \vec{b}_\perp, Y)$.

To find $N(\vec{x}_\perp, \vec{b}_\perp, Y)$ let us consider the following (Glauber) model. Assume that the nucleus is very large and dilute and is made out of $A \gg 1$ independent nucleons, where A is

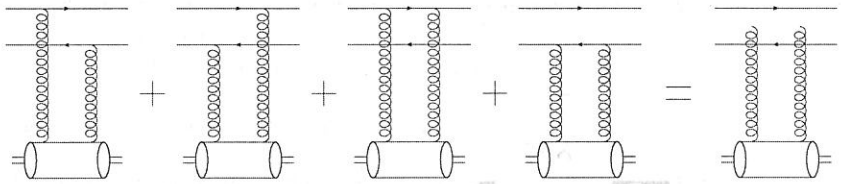

Fig. 4.3. The four diagrams contributing to dipole interaction with a single nucleon at the lowest nontrivial (two-gluon) order in the high energy approximation and an abbreviated notation for their sum.

the atomic number of the nucleus.[1] Any correlations between the nucleons are suppressed by powers of the large parameter A: hence our approximation corresponds to summing the leading powers of A. In evaluating the forward dipole–nucleus scattering amplitude $N(\vec{x}_\perp, \vec{b}_\perp, Y)$ we will follow the strategy originally outlined by Glauber and by Gribov (Glauber 1955, Franco and Glauber 1966, Gribov 1969b, Glauber and Matthiae 1970, Gribov 1970) and implemented in QCD by Mueller (1990).

4.2.1 Scattering on one nucleon

First we consider the case when the dipole interacts with only one nucleon in the nucleus. Assuming that the interaction is entirely perturbative, we see that the lowest-order contribution to the forward high energy scattering amplitude comes from a two-gluon exchange. The relevant diagrams are shown in Fig. 4.3. This lowest-order scattering process was calculated in Sec. 3.2. Employing the results of that section (see Eq. (3.25)) we can write down the total dipole–nucleon cross section as

$$\sigma^{q\bar{q}N} \approx \frac{2\pi\alpha_s^2 C_F}{N_c} x_\perp^2 \ln \frac{1}{x_\perp^2 \Lambda^2}. \tag{4.25}$$

In arriving at Eq. (4.25) we have assumed that the dipole is perturbatively small, $x_\perp \ll 1/\Lambda_{QCD}$, and that the nucleon can be modeled as another dipole of transverse size $1/\Lambda \gg x_\perp$, with Λ some soft QCD scale of order Λ_{QCD}. We have also assumed that the nucleus is sufficiently large that the cross section does not depend on the dipole's orientation in the transverse plane, over which we therefore average.

At the same two-gluon order the unintegrated gluon distribution function of the nucleon can be found using Eq. (3.92) with the lowest-order BFKL Green function (3.59). This gives

$$\phi_{LO}^{onium}(x, k_\perp^2) = \frac{\alpha_s C_F}{\pi} \frac{2}{k_\perp^2}, \tag{4.26}$$

where we have assumed that $k_\perp \gg \Lambda$. The factor 2 on the right-hand side of Eq. (4.26) simply counts the number of quarks in the dipole representing the nucleon. It should be

[1] Strictly speaking A is called the mass number of the nucleus; nevertheless, we will follow the standard jargon in the high energy field and refer to it as the atomic number.